

COSMIC STAR FORMATION HISTORY AND THE FUTURE OBSERVATION OF SUPERNOVA RELIC NEUTRINOS

SHIN'ICHIRO ANDO

Department of Physics, School of Science, The University of Tokyo, 7-3-1 Hongo, Bunkyo-ku, Tokyo 113-0033, Japan

Submitted 2003 November 17; revised 2004 January 19

ABSTRACT

We investigate the flux and event rate of supernova relic neutrinos (SRN), and discuss their implications for the cosmic star formation rate. Since SRN is diffuse neutrino background emitted from past core-collapse supernova explosions, it contains fruitful information on supernova rate in the past and present universe as well as the supernova neutrino spectrum itself. As reference models, we adopt the supernova rate model based on recent observations, and supernova neutrino spectrum numerically calculated by several groups. In the detection energy range $E_e > 10$ MeV, which will possibly be a background free region in the near future, the SRN event rate is found to be $1\text{--}2 \text{ yr}^{-1}$ at the water Čerenkov detector with fiducial volume of 22.5 kton, depending on the adopted neutrino spectrum. We also simulate the expected signal with one set of the reference models, by using the Monte Carlo method, and then analyze these pseudo-data with several free parameters, obtaining distribution of the best fit values for them. In particular, we use parametrization such that $R_{\text{SN}}(z) = R_{\text{SN}}^0(1+z)^\alpha$, where $R_{\text{SN}}(z)$ is the comoving supernova rate density at redshift z and R_{SN}^0, α are free parameters, assuming the supernova neutrino spectrum and luminosity are well understood by a future galactic supernova neutrino burst or future development of the numerical supernova simulation. The obtained 1σ errors for these two parameters are found to be $\delta\alpha/\langle\alpha\rangle = 30\%$ (7.8%) and $\delta R_{\text{SN}}^0/\langle R_{\text{SN}}^0 \rangle = 28\%$ (7.7%) for the detector with an effective volume of $22.5 \text{ kton} \cdot 5 \text{ yr}$ (440 kton \cdot 5 yr), in the case of the other parameter is fixed. On the other hand, if we fix neither values for these two parameters, the expected errors become rather large as $\delta\alpha/\langle\alpha\rangle = 37\%$ and $\delta R_{\text{SN}}^0/\langle R_{\text{SN}}^0 \rangle = 55\%$ even with effective volume of 440 kton \cdot 5 yr.

Subject headings: diffuse radiation — neutrinos — galaxies: evolution — supernovae: general

1. INTRODUCTION

In recent years, we have made remarkable progress in our knowledge concerning how the cosmic star formation history proceeded in the past and concerning the fraction of baryons locked up in stars and gas in the local universe. These points were inferred from observations of the light emitted by stars of various masses at various wavelengths. Madau et al. (1996) investigated the galaxy luminosity density of rest-frame ultraviolet (UV) radiation up to $z \sim 4$, and they converted it into the cosmic star formation rate (SFR). The rest-frame UV light is considered to be a direct tracer of star formation because it is mainly radiated by short-lived massive stars. After the pioneering study by Madau et al., a wealth of data have become available in the form of cosmic SFR in a wide range of redshift; these data were inferred from observations using far infrared (FIR)/submm dust emission (Hughes et al. 1998; Flores et al. 1999) and near infrared (NIR) H α line (Gallego et al. 1995; Gronwall 1998; Tresse & Maddox 1998; Glazebrook et al. 1999) as well as the rest-frame UV emission from massive stars (Lilly et al. 1996; Cowie et al. 1996; Connolly et al. 1997; Sawicki, Lin, & Yee 1997; Treyer et al. 1998; Madau, Pozzetti, & Dickinson 1998b; Pascale, Lanzetta, & Fernandez-Soto 1998; Steidel et al. 1999).

In these traditional methods, however, there are a fair amount of ambiguities when the actual observables are converted into the cosmic SFR (Somerville, Primack, & Faber 2001). First, observable samples are generally flux-limited, and thus the intrinsic luminosity of the faintest objects in the sample changes with redshift. In order to understand the true redshift dependence of the total luminosity density, this incompleteness is generally corrected by using a functional form (i.e., a Schechter function) to the luminosity function ob-

tained from the observations themselves. Unfortunately, since the luminosity function is not well established observationally (especially for high- z region), it is uncertain whether the Schechter-function fit is sufficiently good or not. Secondly, the conversion from luminosity density to SFR generally relies on stellar population models, an assumed star formation history, and initial mass function (IMF), which are not also well established yet. Lastly, if the tracer of star formation is an optical or UV luminosity, then the effects of dust extinction are non-negligible. Although this problem is less critical in other wavebands such as NIR H α or FIR/submm, the bulk of current data is consist of the rest-frame UV observations especially at high redshift region. After adopting some correction law of dust extinction, the rest-frame UV data become rather consistent with H α or submm data points; still in this case, it is unknown whether the UV and submm sources are identical, which is very important for measuring the cosmic SFR.

Thus, our knowledge concerning the cosmic SFR is quite crude, and then another observation which is independent of the above methods will have very important meaning. In this paper, we consider supernova relic neutrinos (SRN), i.e., a diffuse background of neutrinos which were emitted from past supernova explosions. Type Ib, Ic, and II supernova explosions are considered to have traced the cosmic SFR, because they are directly connected with the death of massive stars with $M \gtrsim 8M_\odot$, and their lifetime is expected to be very short compared with the time scale of star formation. These events are triggered by gravitational collapse, and 99% of the gravitational binding energy is released as neutrinos; this basic scenario was roughly confirmed by the well-known observation of neutrino burst from SN 1987A by the Kamiokande-II and IMB detectors (Hirata et al. 1987; Bionta et al. 1987). Advantages of using SRN in order to probe the cosmic SFR

are as follows. First, as already mentioned above, if we can probe the supernova rate from the SRN observation, it can be directly transformed to SFR assuming IMF, because supernovae are short-lived astrophysical events. The second advantage, which will be more important, is that neutrinos are completely free from dust extinction. This point is the same as the observation in submm waveband, however, neutrinos are emitted directly from stars; on the other hand, submm radiation comes from dust itself and it is an indirect process.

The SRN flux and the event rate at a currently working large volume water Čerenkov detector, Super-Kamiokande (SK), were investigated by many researchers using theoretically/observationally modeled SFR (Totani & Sato 1995; Totani, Sato, & Yoshii 1996; Malaney 1997; Hartmann & Woosley 1997; Kaplinghat, Steigman, & Walker 2000; Ando, Sato, & Totani 2003). More recently, the SK collaboration obtained the 90% C.L. upper limit on the SRN flux, i.e., $< 1.2 \text{ cm}^{-2} \text{ s}^{-1}$ in the energy range of $E_\nu > 19.3 \text{ MeV}$ (Malek et al. 2003). This severe constraint is only about factor 3–6 larger than the typical theoretical models, and is very useful to obtain several rough implications for the cosmic SFR (Fukugita & Kawasaki 2003; Strigari et al. 2003) and neutrino properties as elementary particles (Ando & Sato 2003a; Ando 2003).

However, we need further ~ 40 years to reduce the current limit by a factor of 3, if we use the SK detector with current performance. This is because there is no energy window for the SRN detection, in which the SRN signal dominates the other background events coming from various sources, such as solar, reactor, and atmospheric neutrinos, as well as cosmic-ray muons (Ando et al. 2003). Therefore, the current observation is seriously affected by the other backgrounds and takes much time to reach the required sensitivity. In order to overcome this difficulty, a very interesting and promising method was proposed to directly tag electron antineutrinos ($\bar{\nu}_e$), and it is now in the R&D phase (Beacom & Vagins 2003). Their basic idea is to dissolve 0.2% gadolinium trichloride (GdCl_3) into pure-water of SK. With this admixture, 90% of neutrons, produced by $\bar{\nu}_e p \rightarrow e^+ n$ reaction, are captured on Gd and then decays with 8 MeV gamma cascades. When we detect this gamma cascades as well as the preceding Čerenkov radiation from the positron, it indicates these signals come from original $\bar{\nu}_e$, not from other flavor neutrinos or muons. With this method, we can remove the background signals in the energy range 10–30 MeV, in which before removal there are a huge amount of background by solar neutrinos (ν_e) and atmospheric muon-neutrinos ($\nu_\mu, \bar{\nu}_\mu$) or cosmic-ray muon induced events. Because the expected SRN rate is estimated to be $1\text{--}2 \text{ yr}^{-1}$ in the energy range 10–30 MeV, the Gd-loaded SK detector (Gd-SK) would enable us to detect a few SRN events each year.

Therefore, it is obviously important and urgent to give a detailed investigation on the performance of such future detectors. In this paper, we focus on how far we can probe the cosmic supernova rate by the SRN observation at Gd-SK, and hypothetical Gd-loaded Hyper-Kamiokande (Gd-HK) detector or Gd-loaded Underground Nucleon decay and Neutrino Observatory (Gd-UNO). Because the expected event rate of SRN is about $1\text{--}2 \text{ yr}^{-1}$ in the detectable energy range (10–30 MeV) using the detector with the size of SK, it would be quite difficult to obtain the spectral information of SRN, even though we did observation for 5 years. On the other hand, with the currently proposed mega-ton class detectors such as HK and UNO, we can expect to obtain rich information about

the SRN spectrum, which will be useful to infer the SFR- z relation. Using the Monte Carlo (MC) method, we simulate an expected SRN signal at these future detectors, then we analyze those hypothetical data with a few free parameters, and discuss implications from the future SRN observation.

This paper is organized as follows. In §2, we give formulation for calculating the SRN flux and discuss several models which are adopted in our calculations, and in §3, we show results of our calculation with some reference models. In §4, the MC simulation of the expected signal at the future Gd-loaded detectors, which is generated from the reference models, is presented, and then we analyze these hypothetical data using several free parameters concerning the cosmic SFR. Finally, we discuss other possibilities in §5.

2. FORMULATION AND MODELS

2.1. Formulation

The present number density of SRN ($\bar{\nu}_e$), whose energy is in the interval of $E_\nu \sim E_\nu + dE_\nu$, emitted in the interval of the redshift $z \sim z + dz$ is given by

$$\begin{aligned} dN_\nu(E_\nu) &= R_{\text{SN}}(z)(1+z)^3 \frac{dt}{dz} \frac{dN_\nu(E'_\nu)}{dE'_\nu} dE'_\nu \\ &\quad \times (1+z)^{-3} \\ &= R_{\text{SN}}(z) \frac{dt}{dz} \frac{dN_\nu(E'_\nu)}{dE'_\nu} (1+z) dE_\nu, \end{aligned} \quad (1)$$

where $E'_\nu = (1+z)E_\nu$ is the energy of neutrinos at redshift z , which is now observed as E_ν ; $R_{\text{SN}}(z)$ represents supernova rate per comoving volume at z , and hence the factor $(1+z)^3$ should be multiplied to obtain the rate per physical volume at that time; dN_ν/dE_ν is the number spectrum of neutrinos emitted by one supernova explosion; and the factor $(1+z)^{-3}$ comes from the expansion of the universe. The Friedmann equation gives the relation between t and z as

$$\frac{dz}{dt} = -H_0(1+z)\sqrt{(1+\Omega_m z)(1+z)^2 - \Omega_\Lambda(2z+z^2)}, \quad (2)$$

and we adopt the standard Λ CDM cosmology ($\Omega_m = 0.3, \Omega_\Lambda = 0.7, H_0 = 70 \text{ } h_{70} \text{ km s}^{-1} \text{ Mpc}^{-1}$).¹ We now obtain the differential number flux of SRN, dF_ν/dE_ν , using the relation $dF_\nu/dE_\nu = c dN_\nu/dE_\nu$:

$$\begin{aligned} \frac{dF_\nu}{dE_\nu} &= \frac{c}{H_0} \int_0^{z_{\text{max}}} R_{\text{SN}}(z) \frac{dN_\nu(E'_\nu)}{dE'_\nu} \\ &\quad \times \frac{dz}{\sqrt{(1+\Omega_m z)(1+z)^2 - \Omega_\Lambda(2z+z^2)}}, \end{aligned} \quad (3)$$

where we assume that gravitational collapses began at the redshift $z_{\text{max}} = 5$.

2.2. Model for Cosmic Star Formation Rate

As our reference model for SFR, we adopt one which is based on recent progressive results of rest-frame UV, NIR $\text{H}\alpha$, and FIR/submm observations; a simple functional form for the SFR per unit comoving volume is given as (Porciani & Madau 2001)

$$\begin{aligned} \psi_*(z) &= 0.32 h_{70} \frac{\exp(3.4z)}{\exp(3.8z) + 45} M_\odot \text{ yr}^{-1} \text{ Mpc}^{-3} \\ &\quad \times \frac{\sqrt{(1+\Omega_m z)(1+z)^2 - \Omega_\Lambda(2z+z^2)}}{(1+z)^{3/2}}. \end{aligned} \quad (4)$$

¹ Although we use the specific cosmological model here, the SRN flux itself is completely independent of such cosmological parameters, as long as we use observationally inferred SFR models (see their cancellation between eqs. [3] and [4]), as already discussed in Ando et al. (2003).

Figure 1 shows the SFR $\psi_*(z)$ with the various data points by rest-frame UV (Lilly et al. 1996; Madau et al. 1996; Steidel et al. 1999), H α line (Gallego et al. 1995; Gronwall 1998; Tresse & Maddox 1998), and FIR/submm (Flores et al. 1999; Hughes et al. 1998) observations; these data points are not corrected for dust extinction. In the local universe, all studies

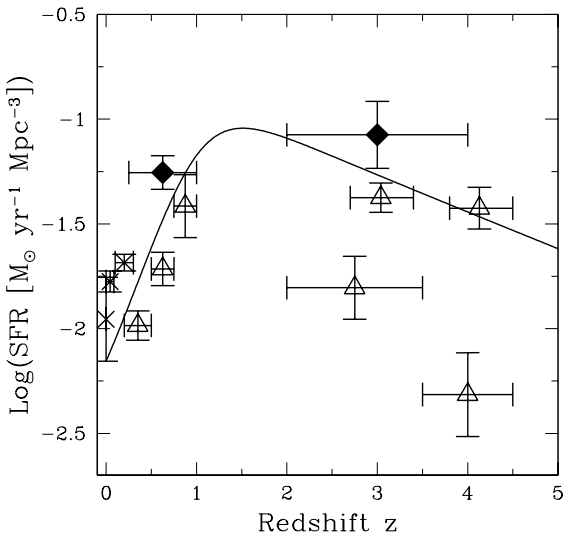


FIG. 1.— Cosmic star formation rate as a function of redshift. Data points are given by rest-frame UV (open triangles; Lilly et al. 1996; Madau et al. 1996; Steidel et al. 1999), NIR H α (crosses; Gallego et al. 1995; Gronwall 1998; Tresse & Maddox 1998), and FIR/submm (filled diamonds; Flores et al. 1999; Hughes et al. 1998) observations. The solid curve represents our reference model given by equation (4). The standard Λ CDM cosmology is adopted ($\Omega_m = 0.3, \Omega_\Lambda = 0.7, H_0 = 70 \text{ km s}^{-1} \text{ Mpc}^{-1}$)

show that the comoving SFR monotonically increases with z out to a redshift of at least 1. Our reference model (4) is consistent with mildly dust corrected UV data at low redshift, on the other hand it may underestimate the results of the other waveband observations. In our previous paper (Ando et al. 2003), we investigated the dependence on the several adopted SFR models, which were only different at high redshift region ($z \gtrsim 1.5$); our reference model (4) was referred to as the “SF1” model there. We showed that the SRN flux at $E_\nu > 10 \text{ MeV}$ is highly insensitive to the difference among the SFR models (owing to the energy redshift as discussed in §3.1), and therefore, we do not repeat such discussions in the present paper.

We obtain the supernova rate ($R_{\text{SN}}(z)$) from the SFR by assuming the Salpeter IMF ($\phi(m) \propto m^{-2.35}$) with lower cutoff around $0.5M_\odot$, and that all stars with $M > 8M_\odot$ explode as core-collapse supernovae, i.e.,

$$R_{\text{SN}}(z) = \frac{\int_{8M_\odot}^{125M_\odot} dm \phi(m)}{\int_0^{125M_\odot} dm m\phi(m)} \psi_*(z) = 0.0122M_\odot^{-1} \psi_*(z). \quad (5)$$

The resulting local supernova rate agrees within errors with the observed value of $R_{\text{SN}}(0) = (1.2 \pm 0.4) \times 10^{-4}h_{70}^3 \text{ yr}^{-1} \text{ Mpc}^{-3}$ (e.g., Madau, della Valle, & Panagia 1998a, and references therein). In fact, totally time-integrated neutrino spectrum from massive stars ($\gtrsim 30M_\odot$) could be very

different from the models we use (and give in the next subsection), possibly because of e.g., a black hole formation. However, the conversion factor appeared in equation (5) is highly insensitive to the upper limit of the integral in the numerator; for instance, if we change the upper limit in the numerator to $25M_\odot$, the factor becomes $0.010M_\odot^{-1}$, which is only slightly different from the value in equation (5).

2.3. Neutrino Spectrum from Supernova Explosions

As neutrino spectrum from each supernova, we adopt three reference models by different groups, i.e., simulations by the Lawrence Livermore group (Totani et al. 1998) and Thompson, Burrows, & Pinto (2003), and the MC study of spectral formation by Keil, Raffelt, & Janka (2003). In this field, however, the most serious problem is that the recent sophisticated hydrodynamical simulations have not obtained the supernova explosion itself, i.e., shock wave cannot penetrate the entire core. Therefore, many points still remain controversial, e.g., the average energy ratio among different flavor neutrinos, or how the gravitational binding energy is distributed to each flavor. All these problems are quite serious for our estimation, since the released binding energy as $\bar{\nu}_e$ changes the normalization of the SRN flux, and the average energy affects the SRN spectral shape. Thus, we believe that these three models from different groups will be complementary to each other.

The numerical simulation by the Lawrence Livermore group (LL; Totani et al. 1998) is considered to be the most appropriate for our estimation, because it is the only model that succeeded to obtain a robust explosion and to calculate the neutrino spectrum during the entire burst ($\sim 15 \text{ s}$). According to their calculation, the average energy difference between $\bar{\nu}_e$ and ν_x , where ν_x represent the non-electron flavor neutrinos and antineutrinos, was rather large and the complete equipartition of the binding energy was realized $L_{\nu_e} = L_{\bar{\nu}_e} = L_{\nu_x}$, where L_{ν_α} represents the released gravitational energy as α -flavor neutrinos. Neutrino spectrum obtained by their simulation is well fitted by a simple formula, which was originally given by Keil et al. (2003), as

$$\frac{dN_\nu}{dE_\nu} = \frac{(1+\beta_\nu)^{1+\beta_\nu} L_\nu}{\Gamma(1+\beta_\nu) \bar{E}_\nu^2} \left(\frac{E_\nu}{\bar{E}_\nu} \right)^{\beta_\nu} e^{-(1+\beta_\nu)E_\nu/\bar{E}_\nu}, \quad (6)$$

where \bar{E}_ν is the average energy; the values for fitting parameters of $\bar{\nu}_e$ and ν_x spectrum are summarized in Table 1.

Although the LL group succeeded to obtain the robust explosion, their result is recently criticized because it lacked many relevant neutrino processes which are recognized to be important in these days. Thus, we adopt the recent result of another hydrodynamical simulation by Thompson et al. (2003) (TBP), which included all the relevant neutrino processes such as neutrino bremsstrahlung as well as neutrino-nucleon scattering with nucleon recoil. Their calculation obtained no explosion, and the neutrino spectrum ends at 0.25 s after core bounce. In the strict sense, we cannot use their result as our reference model because the fully time-integrated neutrino spectrum is definitely necessary in our estimate. However, we adopt their result in order to confirm the effect of recent sophisticated treatment for neutrino processes in supernova core on the SRN spectrum. The TBP calculations include three progenitor mass model, i.e., 11, 15, and $20M_\odot$; all of these models are also well fitted by equation (6) and the fitting parameters are summarized in Table 1. The average energy for both $\bar{\nu}_e$ and ν_x is much smaller than that by the LL calculation. Although we did not show in Table 1, it was also

TABLE 1. FITTING PARAMETERS FOR SUPERNOVA NEUTRINO SPECTRUM

Model	Mass (M_{\odot})	$\bar{E}_{\bar{\nu}_e}$ (MeV)	\bar{E}_{ν_x} (MeV)	$\beta_{\bar{\nu}_e}$	β_{ν_x}	$L_{\bar{\nu}_e}$ (erg)	L_{ν_x} (erg)	Reference
LL	20	15.4	21.6	3.8	1.8	4.9×10^{52}	5.0×10^{52}	1
TBP	11	11.4	14.1	3.7	2.2	2
	15	11.4	14.1	3.7	2.2	2
	20	11.9	14.4	3.6	2.2	2
KRJ	...	15.4	15.7	4.2	2.5	3

REFERENCES. — (1) Totani et al. 1998; (2) Thompson et al. 2003; (3) Keil et al. 2003.

found that at least for the early phase of the core-collapse, the complete equipartition of the gravitational binding energy to each flavor was not realized. However, it is quite unknown whether these trends hold during the entire burst. In this study, as our reference model we adopt the average energy given in Table 1, while we assume perfect equipartition between flavors, i.e., $L_{\bar{\nu}_e} = L_{\nu_x} = 5.0 \times 10^{52}$ erg.

In addition, we also use the model by Keil et al. (2003) (KRJ). Their calculation did not couple with the hydrodynamics, but it focused on the spectral formation of each flavor neutrino using MC simulation. Therefore, the static model was assumed as background of neutrino radiation, and we use their “accretion phase model II,” in which the neutrino transfer was solved in the background of 150 ms post-bounce model from a general relativistic simulation. The fitting parameters for their MC simulation is also summarized in Table 1. Unlike the previous two calculations, their result clearly shows that the average energy of ν_x is very close to that of $\bar{\nu}_e$. It also indicates that the equipartition among each flavor was not realized but $L_{\nu_e} \simeq L_{\bar{\nu}_e} \simeq 2L_{\nu_x}$. However also in this case, since the totally time-integrated neutrino flux is unknown from such temporary information, we assume perfect equipartition, $L_{\bar{\nu}_e} = L_{\nu_x} = 5.0 \times 10^{52}$ erg as well as that the average energies are the same as those in Table 1.

2.4. Neutrino Spectrum after Neutrino Oscillation

The original $\bar{\nu}_e$ spectrum is different from that we observe as $\bar{\nu}_e$ at the Earth, owing to the effect of neutrino oscillation. Since the specific flavor neutrinos are not mass eigenstates, they mixes with other flavor neutrinos during their propagation. The behavior of flavor conversion inside the supernova envelope is well understood, because the relevant mixing angles and mass square differences are fairly well determined by recent solar, atmospheric, and reactor neutrino experiments. The remaining ambiguities concerning the neutrino oscillation parameters are the value of θ_{13} , which is only weakly constrained ($\sin^2 \theta_{13} \lesssim 0.1$; Apollonio et al. 1999), and the type of mass hierarchy, i.e., normal ($m_1 \ll m_3$) or inverted ($m_1 \gg m_3$). For a while, we discuss the case of normal mass hierarchy as our standard model; in this case, the value of θ_{13} is irrelevant. The case of inverted mass hierarchy is addressed in §5.3. In addition, other exotic mechanisms, such as resonant spin-flavor conversion (see Ando & Sato 2003b, and references therein) and neutrino decay (Ando 2003), which possibly change the SRN flux and spectrum, might work in reality. However, we do not consider such possibilities in this study.

The produced $\bar{\nu}_e$ at the supernova core are coincident with the lightest mass eigenstate $\bar{\nu}_1$ owing to the large matter potentials. Since this state $\bar{\nu}_1$ is the lightest also in vacuum, there

are no resonance regions, in which one mass eigenstate can change into another state, and therefore $\bar{\nu}_e$ at production arrives at the stellar surface as $\bar{\nu}_1$. Thus, the observed $\bar{\nu}_e$ spectrum by the distant detector is

$$\begin{aligned} \frac{dN_{\bar{\nu}_e}}{dE_{\bar{\nu}_e}} &= |U_{e1}|^2 \frac{dN_{\bar{\nu}_1}}{dE_{\bar{\nu}_1}} + |U_{e2}|^2 \frac{dN_{\bar{\nu}_2}}{dE_{\bar{\nu}_2}} + |U_{e3}|^2 \frac{dN_{\bar{\nu}_3}}{dE_{\bar{\nu}_3}} \\ &= |U_{e1}|^2 \frac{dN_{\bar{\nu}_e}^0}{dE_{\bar{\nu}_e}} + (1 - |U_{e1}|^2) \frac{dN_{\nu_x}^0}{dE_{\nu_x}}, \end{aligned} \quad (7)$$

where the quantities with superscript 0 represent those at production, $U_{\alpha i}$ is the mixing matrix element between α -flavor state and i -th mass eigenstate, and observationally $|U_{e1}|^2 = 0.7$. In other words, 70% of the original $\bar{\nu}_e$ survives, on the other hand, the remaining 30% comes from the other component ν_x . Therefore, both the original $\bar{\nu}_e$ and ν_x spectra are necessary for the estimation of the SRN flux and spectrum; since the original ν_x spectrum is generally harder than that of original $\bar{\nu}_e$ as shown in Table 1, the flavor mixing is expected to harden the detected SRN spectrum.

3. FLUX AND EVENT RATE OF SUPERNOVA RELIC NEUTRINOS

3.1. Flux of Supernova Relic Neutrinos

The SRN flux can be calculated by equation (3) with our reference models given in §2. Figure 2 shows the SRN flux as a function of neutrino energy for the three supernova models, LL, TBP, and KRJ. The flux of atmospheric $\bar{\nu}_e$, which becomes background events of the SRN detection is also shown in the same figure (Gaisser, Stanev, & Barr 1988; Barr, Gaisser, & Stanev 1989). The SRN flux peaks at $\lesssim 5$ MeV and around this peak, the TBP model gives the largest SRN flux because the average energy of original $\bar{\nu}_e$ is considerably smaller than the other two models, but the total luminosity is assumed to be the same. On the other hand, it gives smaller contribution at high energy region, $E_{\nu} > 10$ MeV. In contrast, the high energy tail of the SRN flux with the LL model extends farther than that with the other models, and it gives more than one magnitude larger flux at $E_{\nu} = 60$ MeV. This is because the high energy tail was mainly contributed by the harder component of the original neutrino spectrum; in the case of the LL calculation, the average energy of the harder component ν_x is significantly larger than that of the other two calculations as shown in Table 1. We show the values of the SRN flux integrated over the various energy ranges in Table 2. (For a while, we refer to the upper part of the table just as Table 2, while the values in the lower part are discussed later in §5.3.) The total flux is expected to be $11\text{--}16 \text{ cm}^{-2} \text{ s}^{-1}$ for our reference models, although this value is quite sensitive to the shape of assumed SFR, especially at high- z . The energy range in which we are more interested is high energy

TABLE 2. FLUX AND EVENT RATE OF SUPERNOVA RELIC NEUTRINOS

Model	Redshift Range	Flux [cm ⁻² s ⁻¹]			Event Rate [(22.5 kton yr) ⁻¹]	
		Total	$E_\nu > 11.3$ MeV	$E_\nu > 19.3$ MeV	$E_e > 10$ MeV	$E_e > 18$ MeV
LL	Total	11.7	2.3	0.46	2.3	1.0
	$0 < z < 1^a$	4.1 (35.3)	1.6 (70.9)	0.39 (85.2)	1.7 (77.5)	0.9 (87.5)
	$1 < z < 2^a$	4.9 (42.0)	0.6 (26.3)	0.06 (14.0)	0.5 (20.6)	0.1 (11.9)
	$2 < z < 3^a$	1.8 (15.1)	0.1 (2.5)	0.0 (0.7)	0.0 (1.7)	0.0 (0.5)
	$3 < z < 4^a$	0.6 (5.3)	0.0 (0.2)	0.0 (0.0)	0.0 (0.1)	0.0 (0.0)
	$4 < z < 5^a$	0.2 (2.1)	0.0 (0.0)	0.0 (0.0)	0.0 (0.0)	0.0 (0.0)
TBP	Total	16.1	1.3	0.14	0.97	0.25
KRJ	Total	12.7	2.0	0.28	1.7	0.53
Inverted Mass Hierarchy with Large θ_{13}						
LL	Total	9.4	3.1	0.94	3.8	2.3
TBP	Total	13.8	1.9	0.30	1.6	0.58
KRJ	Total	12.4	2.2	0.38	2.0	0.76

NOTE. — Values in the upper part are evaluated for the case of normal mass hierarchy (or inverted mass hierarchy with sufficiently small θ_{13} , i.e., $\sin^2 2\theta_{13} \lesssim 10^{-5}$), which we use as our standard model. On the other hand, values in the lower part are applicable only when the value of θ_{13} is large enough to induce completely adiabatic resonance, i.e., $\sin^2 2\theta_{13} \gtrsim 10^{-3}$, in the case of inverted mass hierarchy.

^aContributions from each redshift range to the total ($0 < z < 5$) value are shown in parentheses in unit of %.

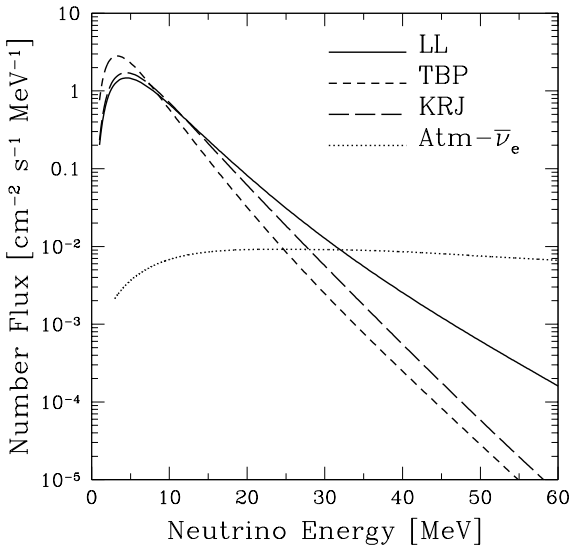


FIG. 2.— SRN flux calculated with three reference models of original neutrino spectrum, LL (Totani et al. 1998), TBP (Thompson et al. 2003), and KRJ (Keil et al. 2003). The flux of atmospheric neutrinos (Gaisser et al. 1988; Barr et al. 1989) is also shown for comparison.

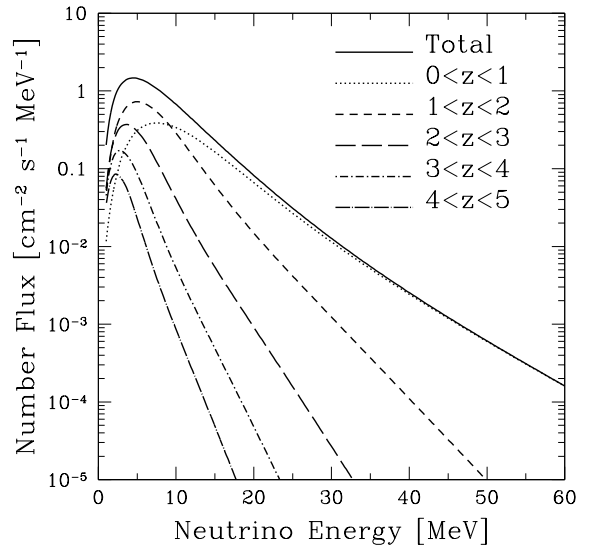


FIG. 3.— SRN flux from various redshift ranges. As the supernova model, LL is adopted.

region such as $E_\nu > 19.3$ MeV and $E_\nu > 11.3$ MeV, because as discussed below the background events are less critical as well as that the reaction cross section increases as $\propto E_\nu^2$. In such a range, the SRN flux is found to be $1.3\text{--}2.3$ cm⁻² s⁻¹ ($E_\nu > 11.3$ MeV) and $0.14\text{--}0.46$ cm⁻² s⁻¹ ($E_\nu > 19.3$ MeV). Thus, the uncertainty about the supernova neutrino spectrum and its luminosity gives at least a factor 2–4 ambiguity to the expected SRN flux in the energy region of our interest.

Figure 3 shows the contribution by supernova neutrinos emitted from various redshift ranges. At high energy region $E_\nu > 10$ MeV, the dominant flux comes from the local supernovae ($0 < z < 1$), while the low energy side is mainly con-

tributed by the high redshift events ($z > 1$). This is because the energy of neutrinos, which were emitted from a supernova at redshift z , is reduced by a factor of $(1+z)^{-1}$ reflecting the expansion of the universe, and therefore, high redshift supernovae only contribute to low energy flux. We also show the energy integrated flux from each redshift range in Table 2 in the case of the LL supernova model. From the table, it is found that in the energy range of our interest, more than 70% flux comes from the local supernova explosions as $z < 1$, while the high redshift ($z > 2$) supernova contribution is very little.

3.2. Event Rate at Water Čerenkov Detectors

The water Čerenkov neutrino detectors have greatly succeeded to probe the neutrino properties as an elementary particle, such as neutrino oscillation. The SK detector is one of such detectors, and its large fiducial volume (22.5 kton) might enable us to detect the diffuse background of supernova neutrinos (SRN). Furthermore, much larger water Čerenkov detectors such as HK and UNO are planned presently. The SRN detection is the most probable with the inverse beta-decay reaction with protons in water, $\bar{\nu}_e p \rightarrow e^+ n$, and its cross section is precisely understood (Vogel & Beacom 1999; Strumia & Vissani 2003). In our calculation, we use the trigger threshold of SK-I (before the accident).

The expected event rate at such detectors are shown in Figs. 4 and 5 in unit of $(22.5 \text{ kton yr})^{-1} \text{ MeV}^{-1}$; with SK, it takes a year to obtain the shown SRN spectrum, while with HK and UNO, much less time ($1 \text{ yr} \times [22.5 \text{ kton}/V_{\text{fid}}]$, where V_{fid} is the fiducial volume of HK or UNO) is necessary because of their larger fiducial volume. Figure 4 compares the three models

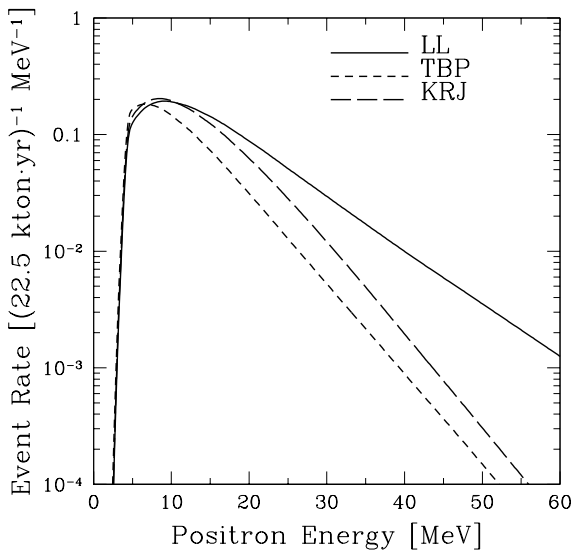


FIG. 4.— Event rate at water Čerenkov detectors in unit of $(22.5 \text{ kton yr})^{-1}$, for three supernova models.

of original supernova neutrino spectrum, and Fig. 5 shows the contribution to the total event rate from each redshift range. In Table 2, we summarize the event rate integrated over various energy ranges for three supernova models. The expected event rate is $0.97\text{--}2.3$ $(22.5 \text{ kton yr})^{-1}$ for $E_e > 10$ MeV and $0.25\text{--}1.0$ $(22.5 \text{ kton yr})^{-1}$ for $E_e > 18$ MeV. This clearly indicates that if the background events which hinder the detection is negligible, the SK has already reached required sensitivity to detect SRN; with the future HK and UNO, the statistically significant discussion would be accessible. It also shows that the current shortage of our knowledge concerning the original supernova neutrino spectrum and luminosity gives at least a factor 2 ($E_\nu > 10$ MeV) to 4 ($E_\nu > 18$ MeV) uncertainty to the event rate at high energy range (actual detection range). We also summarize the contribution from each redshift range in the same table especially for the calculation with the LL model. The bulk of the detected events will come from the local universe ($z < 1$), but the considerable flux is potentially attributed to the range of $1 < z < 2$.

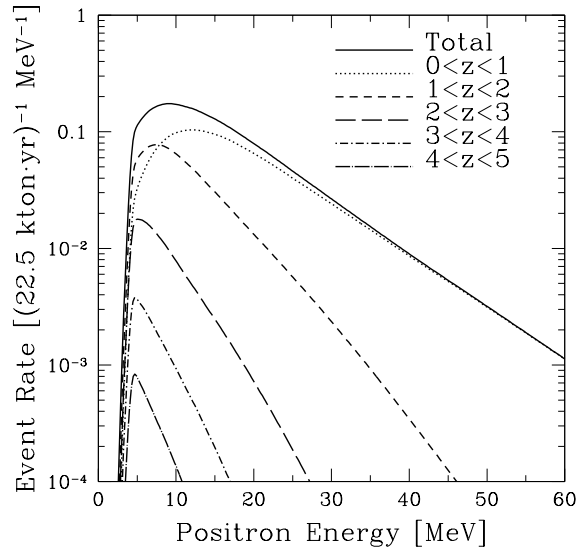


FIG. 5.— Event rate at water Čerenkov detectors in unit of $(22.5 \text{ kton yr})^{-1}$, from various redshift ranges. As the supernova model, LL is adopted.

3.3. Comparison with Other Studies and Current Observational Limit

There are many past theoretical researches concerning the SRN flux estimation based on theoretically/observationally modeled cosmic SFR (Totani et al. 1996; Malaney 1997; Hartmann & Woosley 1997; Ando et al. 2003). Here, we briefly compare our results obtained in §3.1 and §3.2 with these past analyses. Our basic approach in the present paper is the same as that in Ando et al. (2003), in which the LL supernova model was adopted. Thus the values for the LL model given in Table 2 is almost the same as those in Ando et al. (2003). Other two studies (Totani et al. 1996; Hartmann & Woosley 1997) also used similar SFR- z relation at low redshift, and therefore, their results are very well consistent with the present one (the LL model) at high energy region $E_\nu > 10$ MeV. Since the SFR model adopted by Malaney (1997) gave rather lower value at low redshift, the resulting SRN flux at high energy region was about a factor 2 smaller than our LL model or the other ones (Totani et al. 1996; Hartmann & Woosley 1997; Ando et al. 2003). Thus, our calculation with the LL supernova model gives quite consistent values with past studies within a factor of 2, but all of them used the supernova model that is very similar to the LL model. In fact, the present study is the first one that investigated the dependence on the adopted supernova models, by using various original spectrum by different groups (LL, TBP, and KRJ). As already mentioned in §3.1, it was found that the ambiguity concerning the original neutrino spectrum varies the resulting value of the flux by at least a factor of 2.

In addition, there are several other studies on the SRN flux (Totani & Sato 1995; Kaplinghat et al. 2000; Fukugita & Kawasaki 2003). As for Totani & Sato (1995), the authors used constant supernova rate model in order to investigate the dependence on cosmological parameters; they gave very large value ($\sim 3 \text{ cm}^{-2} \text{ s}^{-1}$ at $E_\nu > 19.3$ MeV), which is already excluded observationally, because they adopted rather large supernova rate. Concerning the other two studies, because both

of them do not give some specific value for the SRN flux, we cannot compare ours with theirs; they focused on giving theoretical upper limit (Kaplinghat et al. 2000) or probing the cosmic SFR with the current observational upper limit by SK (Fukugita & Kawasaki 2003).

Observationally, the SK collaboration gave a very stringent upper limit to the SRN flux at $E_\nu > 19.3$ MeV, i.e., $< 1.2 \text{ cm}^{-2} \text{ s}^{-1}$ (90% C.L.) (Malek et al. 2003). This number can be directly compared with our predictions summarized in Table 2. Our predicted values are 0.46, 0.14, and $0.28 \text{ cm}^{-2} \text{ s}^{-1}$ for the LL, TBP, and KRJ models respectively. Thus, the current SK upper limit is about factor 2.5–8.5 larger than our predictions with the reference model for the cosmic SFR, depending on the adopted original neutrino spectrum.

3.4. Background Events against Detection

In §3.2, we calculated the expected SRN spectrum at the water Čerenkov detectors on the Earth, but the actual detection is quite restricted because of the presence of other background events. They are atmospheric and solar neutrinos, antineutrinos from nuclear reactors, spallation products induced by cosmic ray muons, and decay products of invisible muons (for a detailed discussion of these backgrounds, see Ando et al. 2003). For the pure-water Čerenkov detectors, there is no energy window, in which the flux of any backgrounds is much smaller than the SRN flux.

However, as proposed by Beacom & Vagins (2003) if we use the Gd-loaded detectors, the range 10–30 MeV would be an energy window because we can positively distinguish the $\bar{\nu}_e$ signal from other backgrounds such as solar neutrinos (ν_e), invisible muon events, and spallation products; this is realized by capturing neutrons which are produced by the $\bar{\nu}_e p$ interactions. Above 30 MeV, the SRN flux becomes smaller than the flux of atmospheric $\bar{\nu}_e$ as shown in Fig. 2; because they are the same flavor it is in principle impossible to distinguish them from the SRN $\bar{\nu}_e$. On the other hand below 10 MeV, the reactor neutrinos ($\bar{\nu}_e$) are the dominant background in the case of SK or HK; because the flux of reactor neutrinos strongly depends on the detector site, it may be possible to further reduce this lower energy cutoff (10 MeV) in the case of UNO.

The neutron capture efficiency by Gd is estimated to be 90% with the proposed 0.2% admixture by mass of GdCl_3 in water (Beacom & Vagins 2003), and subsequently 8 MeV gamma cascade occurs from the excited Gd. The equivalent single electron energy to this cascade was found to be 3–8 MeV by the careful simulation (Hargrove et al. 1995), and with the trigger threshold adopted in SK-I, only about 50% of such cascades can be detected actually. However, it is expected that SK-III, which will begin operations in mid-2006, will trigger at 100% efficiency above 3 MeV, with good trigger efficiency down to 2.5 MeV (Beacom & Vagins 2003). In that case the most of gamma cascades from Gd will be detected with their preceding signal of positrons. From this point on, we assume 100% efficiency as such efficiency; even if we abandon this assumption, it does not affect our physical conclusion, since the relevant quantity representing the detector performance is (fiducial volume) \times (time) \times (efficiency), which we call effective volume.

4. MONTE CARLO SIMULATION FOR FUTURE DETECTOR PERFORMANCE

In this section, we predict the expected signal at the future detectors, such as Gd-SK, Gd-HK, and Gd-UNO, using the MC method with our reference models. These pseudo-

data are then analyzed using several free parameters concerning the SFR. Although we focus on how far the SFR can be probed by the SRN observation, the uncertainty from the supernova neutrino spectrum would give a fair amount of errors. However, this problem can be solved if a supernova explosion occurs in our galaxy; the expected event number is about 5000–10000 at SK, when supernova neutrino burst occurs at 10 kpc, and it will enable a statistically significant discussion concerning the neutrino spectrum from supernova explosions. Even though there are no galactic supernovae in the near future, remarkable development of the supernova simulation can be expected as the growth of computational resources and numerical technique. With such development, the supernova neutrino spectrum and luminosity may be uncovered and the concerning ambiguity is expected to be reduced significantly. Thus in this paper, we assume that the supernova neutrino spectrum is well understood and that our reference models are fairly good representatives of nature; we analyze the SFR alone with several free parameters.

The basic procedure of our method is as follows. (i) We simulate the expected signal (spectrum) at the Gd-loaded detector in the range of 10–30 MeV, assuming there are no background events. In that process, we use our reference models for the generation of the SRN signal (eq. [4] for the SFR and the LL model as neutrino spectrum). (ii) Then, we analyze the SRN spectrum using the maximum likelihood method with two free parameters of the SFR and obtain a set of the best fit values for those parameters; they are concerned with the supernova rate as

$$R_{\text{SN}}(z) = \begin{cases} R_{\text{SN}}^0(1+z)^\alpha, & \text{for } z < 1, \\ 2^\alpha R_{\text{SN}}^0, & \text{for } z > 1, \end{cases} \quad (8)$$

where R_{SN}^0 represents the local supernova rate and α determines the slope of supernova rate evolution. Although it is recognized that the SFR- z relation increases from $z=0$ to $z=1$ from various observation using the light, the actual numbers for the absolute value and the slope of the SFR- z relation is still matter of controversy and the independent confirmation, such as ours, is needed. We assume that the comoving SFR is constant at $z > 1$; even if we change this assumption, the result would be the same because the bulk of the detected event comes from local supernovae. (iii) We do 10^3 such MC simulations, and obtain 10^3 independent sets of best fit parameters. Then we discuss the standard deviation of the distributions of such best fit parameter sets, and implications for the cosmic SFR.

4.1. Performance of the Gd-loaded Super-Kamiokande Detector

In this subsection, we discuss the performance of Gd-SK for 5 years, or effective volume of $22.5 \text{ kton} \cdot 5 \text{ yr}$. Because the expected event number is only ~ 10 , the both parameters, R_{SN}^0 and α , cannot be well determined at once. Therefore, we fix one of those parameters with some value inferred from other observations. First, the value of R_{SN}^0 was fixed to be $1.2 \times 10^{-4} \text{ yr}^{-1} \text{ Mpc}^{-3}$, which was inferred from the local supernova survey (Madau et al. 1998a), and we obtained the distribution of the best fit values of parameter α . Figure 6 shows the expected SRN spectrum; points with error bars represent the result of one MC simulation, and the dashed histogram is the spectrum with the best fit parameter ($\alpha = 2.97$). Thus, from one realization of MC simulation, we obtain one best fit parameter. The result of 10^3 times MC simulations are shown

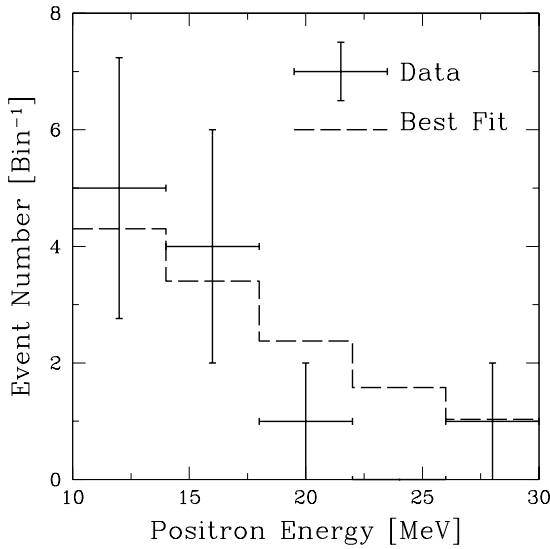


FIG. 6.— Expected SRN spectrum at the detector of effective volume $22.5 \text{ kton} \cdot 5 \text{ yr}$. The data points represent the result of MC simulation and error bars include statistical errors alone. These data generated by MC simulation were analyzed assuming $R_{\text{SN}}^0 = 1.2 \times 10^{-4} \text{ yr}^{-1} \text{ Mpc}^{-3}$, and using α as a free parameter. The best fit value for α is 2.97 and it resulted in dashed histogram in this figure.

in Fig. 7 as a histogram of the distribution of best fit parameters α (solid histogram). The average value of such 10^3 val-

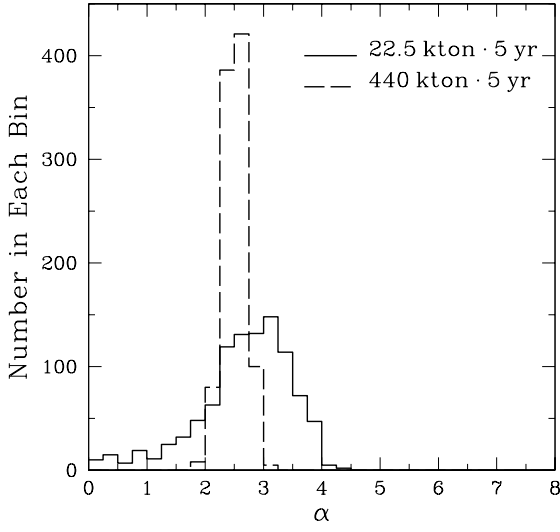


FIG. 7.— Distribution of 10^3 best fit values for α , which are obtained from the analyses of each MC generation. The effective volume is $22.5 \text{ kton} \cdot 5 \text{ yr}$ for solid histogram, and $440 \text{ kton} \cdot 5 \text{ yr}$ for dashed histogram. The value of the local supernova rate is fixed to be $R_{\text{SN}}^0 = 1.2 \times 10^{-4} \text{ yr}^{-1} \text{ Mpc}^{-3}$.

ues for α is found to be 2.67, and the standard deviation 0.80, i.e., $\alpha = 2.67 \pm 0.80$. No evolution (constant supernova rate) model will be excluded at 3.3σ level from the SRN observation alone with effective volume of $22.5 \text{ kton} \cdot 5 \text{ yr}$.

Then in turn, we fixed the value of α to be 2.9 in order to obtain the distribution of best fit values for local supernova rate R_{SN}^0 from the SRN observation. The result of 10^3 MC generations and analyses in this case is shown in Fig. 8. The average

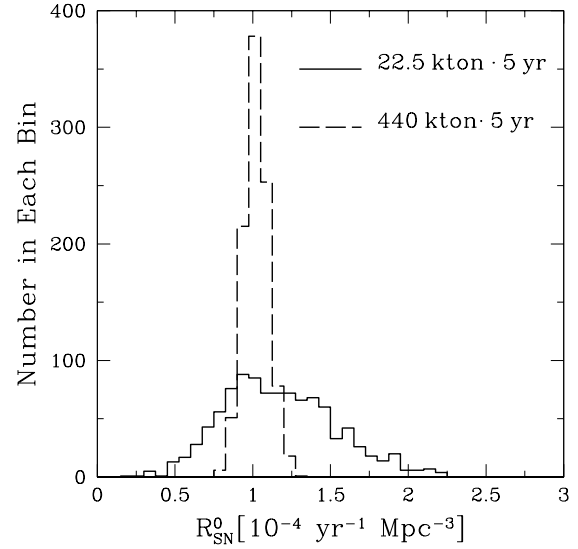


FIG. 8.— Distribution of 10^3 best fit values for local supernova rate R_{SN}^0 , which are obtained from the analyses of each MC generation. The effective volume is $22.5 \text{ kton} \cdot 5 \text{ yr}$ for solid histogram, and $440 \text{ kton} \cdot 5 \text{ yr}$ for dashed histogram. The value of α is fixed to be 2.9.

value for R_{SN}^0 is $1.2 \times 10^{-4} \text{ yr}^{-1} \text{ Mpc}^{-3}$, and the standard deviation $0.4 \times 10^{-4} \text{ yr}^{-1} \text{ Mpc}^{-3}$, i.e., $R_{\text{SN}}^0 = (1.2 \pm 0.4) \times 10^{-4} \text{ yr}^{-1} \text{ Mpc}^{-3}$.

These results obtained by the above calculations are summarized in Table 3. In Fig. 9, we compare the supernova rate model with the parameter inferred from the MC simulations, with the “true” reference model; the cases of fixed R_{SN}^0 and α are shown in Figs. 9(a) and 9(b), respectively. The allowed region at 1σ level is located between two dotted curves, while the solid curve represents our reference model. Thus, with the Gd-SK detector we can roughly reproduce the supernova rate profile at $z < 1$ for 5 years operation, although it is still statistically insufficient.

4.2. Future Gd-loaded Mega-ton Class Detectors

We consider future mega-ton class detectors such as Gd-HK or Gd-UNO. With these detectors, the effective volume that we consider, $440 \text{ kton} \cdot 5 \text{ yr}$, is expected to be realized in several years from the start of their operation. First we did the same analysis adopted in the previous subsection, i.e., we fixed one of relevant parameters, α or R_{SN}^0 , and investigated dependence on the remaining parameter. The values we used for fixed parameters were the same as those given in the previous subsection. The result of those cases are also shown in Figs. 7 and 8 as dashed histograms, which give $\alpha = 2.51 \pm 0.20$ and $R_{\text{SN}}^0 = (1.0 \pm 0.1) \times 10^{-4} \text{ yr}^{-1} \text{ Mpc}^{-3}$, respectively, and these values are also summarized in Table 3. The statistical errors are considerably reduced compared with the case of $22.5 \text{ kton} \cdot 5 \text{ yr}$, because of the ~ 20 times larger effective volume. Thus, future mega-ton detectors possibly pin down, within 10% statistical error, either the index of supernova rate evolution α or local supernova rate R_{SN}^0 if the

TABLE 3. EXPECTED SENSITIVITY OF FUTURE DETECTORS TO SUPERNOVA RATE MODEL

Detector	Effective Volume (22.5 kton yr)	Fixed Parameter	α	$\delta\alpha/\langle\alpha\rangle$ (%)	R_{SN}^0 (10^{-4} yr $^{-1}$ Mpc $^{-3}$)	$\delta R_{\text{SN}}^0/\langle R_{\text{SN}}^0 \rangle$ (%)
SK	5	R_{SN}^0	2.7 ± 0.8	30.0	1.2 (fixed)	...
	5	α	2.9 (fixed)	...	1.2 ± 0.4	28.3
HK or UNO	97.8	R_{SN}^0	2.5 ± 0.2	7.8	1.2 (fixed)	...
	97.8	α	2.9 (fixed)	...	1.0 ± 0.1	7.7
	97.8	...	3.5 ± 1.3	36.7	0.88 ± 0.48	54.8

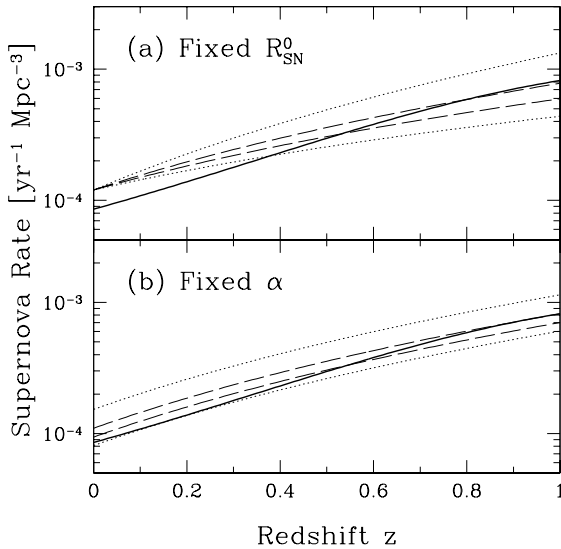


FIG. 9.— Supernova rate as a function of redshift. In both panels, solid curves represent our reference model. (a) The allowed region at 1σ level, concerning the fitting parameter α with fixed R_{SN}^0 , is shown as the area between two dotted (dashed) curves; the effective volume is 22.5 kton \cdot 5 yr (440 kton \cdot 5 yr). (b) The same as (a) but for fitting parameter R_{SN}^0 with fixed α .

other is known in advance. The dashed curves in Fig. 9 set the allowed region of supernova rate at 1σ level by the considered detectors, well reproducing the assumed model.

In principle, we can determine both two parameters by the SRN observation, because R_{SN}^0 is concerned with the absolute value of the flux alone, but α is concerned with both the absolute value and the spectral shape, i.e., these two parameters are not degenerate with each other. Thus, we repeated the same procedure but without fixing the values of α nor R_{SN}^0 . The distribution of 10^3 best fit parameter sets of $(\alpha, R_{\text{SN}}^0)$ is shown in Fig. 10 for the detector with effective volume of 440 kton \cdot 5 yr; the mean values and the standard deviations are $\alpha = 3.5 \pm 1.3$ and $R_{\text{SN}}^0 = (8.8 \pm 4.8) \times 10^{-5}$ yr $^{-1}$ Mpc $^{-3}$. Even though the effective volume is as large as 440 kton \cdot 5 yr, it is still insufficient to determine both parameters at once. For another trial, we also did the same MC simulations, but using hypothetical (and unrealistic) effective volume as large as 440 kton \cdot 10^4 yr. In that case the free parameters are found to be quite well constrained as $\alpha = 3.68 \pm 0.03$ and $R_{\text{SN}}^0 = (7.11 \pm 0.09) \times 10^{-5}$ yr $^{-1}$ Mpc $^{-3}$.

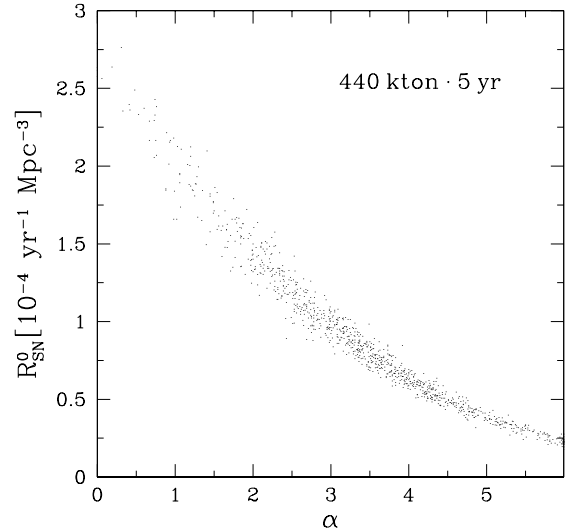


FIG. 10.— Distribution of 10^3 best fit parameter sets $(\alpha, R_{\text{SN}}^0)$. Each dot represents the result of one MC generation and an accompanying analysis. The effective volume is 440 kton \cdot 5 yr.

5. DISCUSSION

5.1. Supernova Rate at High Redshift Region

At the detection energy range 10–30 MeV we have considered, the main contribution to the event rate of SRN comes from low redshift region $0 < z < 1$ as shown in Fig. 5 and Table 2. However, if we can reduce the lower energy threshold E_{th} , it is expected that the contribution of supernova neutrinos from high redshift $z > 1$ becomes enhanced. The value of E_{th} is restricted to be 10 MeV because at further lower energy region there is a large background of reactor neutrinos; its removal is impossible with the current detection method. Since the SK and HK detectors are and will be located at Kamioka in Japan, they are seriously affected by background neutrinos from plenty of nuclear reactors. If some large volume detectors were built at the location free from such a background, the lower threshold energy could be reduced, enabling us to probe the high redshift supernova rate. In this subsection, thus, we discuss the detector performance as a function of the value of E_{th} .

In Fig. 11(a), we show three toy models of comoving density of supernova rate as a function of redshift. These models exactly coincide with each other at $z < 1$ (and also with the

previous reference model represented by eq. [4]), but seriously different at $z > 1$. We calculated the expected event

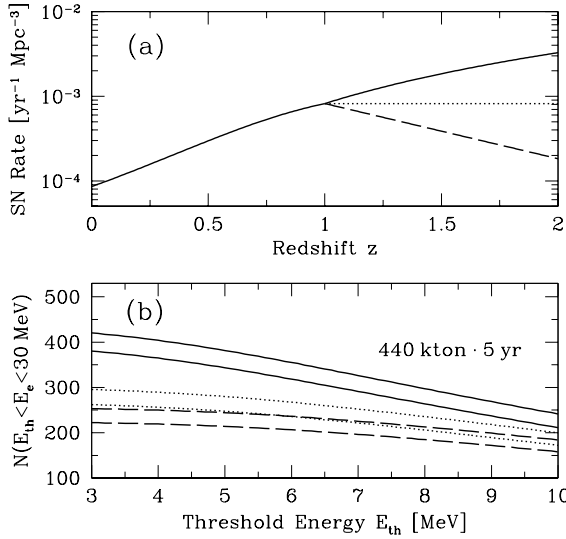


FIG. 11.— (a) Three toy models for comoving density of supernova rate as a function of redshift. (b) Expected event number N at $E_{\text{th}} < E_e < 30 \text{ MeV}$ as a function of E_{th} , for the fiducial volume of $440 \text{ kton} \cdot 5 \text{ yr}$. The line type corresponds to that in the upper panel. Two upper and lower curves represent $N + \sqrt{N}$ and $N - \sqrt{N}$, respectively, i.e., the area between two curves are the allowed region at 1σ level.

number for $E_{\text{th}} < E_e < 30 \text{ MeV}$ at the detector with effective volume of $440 \text{ kton} \cdot 5 \text{ yr}$, using these toy models, the LL spectrum, and trigger threshold expected at SK-III. The result is shown in Fig. 11(b). As expected, the discrepancy among the three models becomes larger as we reduce the threshold energy. In particular, the model which produces larger number of supernovae at $z > 1$ (solid curve) is satisfactorily distinguishable in the case of sufficiently low E_{th} . This is because the larger supernova rate at the high redshift region $z > 1$ increases the fraction of its contribution to the SRN flux. On the other hand, the model with less supernova rate relatively increases the contribution from low redshift region $z < 1$, and therefore the difference between constant (dotted curve) and decreasing model (dashed curve) is less prominent.

5.2. Probing Supernova Neutrino Properties

Until this point, we have assumed that the properties of supernova neutrinos, such as average energy difference between flavors and luminosities of different flavor neutrinos, are quite well understood, when the future SRN detection becomes within reach. However, this assumption itself is quite unclear because galactic supernova explosions, which would give us rich information on the supernova neutrino spectrum and luminosity, may not occur by the time we are ready for the SRN detection. Further, there is no assurance that the numerical experiments succeed obtaining supernova explosion itself and predict the supernova neutrino properties precisely by then. Thus, the SRN observation might be the only probe of the supernova neutrino properties.

In this subsection, we discuss how far we can derive the supernova neutrino properties from the SRN observation. We have already shown that even using data of $440 \text{ kton} \cdot 5 \text{ yr}$,

at most only two free parameters can be satisfactorily constrained. Therefore, we now have to adopt another assumption such that the evolution of supernova rate is quite well understood by future observations with planned various satellites and telescopes. The procedure is basically the same as that of the previous section, i.e., we ran 10^3 MC simulations and analyzed these pseudo-data to obtain the best fit values for two free parameters, $\bar{E}_{\bar{\nu}_e}$ and $\bar{E}_{\nu_x}/\bar{E}_{\bar{\nu}_e}$. The values of β_{ν_e} and L_{ν} defined in equation (6) were assumed to be $\beta_{\bar{\nu}_e} = 4.0$, $\beta_{\nu_x} = 2.2$, and $L_{\bar{\nu}_e} = L_{\nu_x} = 5.0 \times 10^{52} \text{ erg}$. As the result of such calculations, we obtained the distribution of the two parameters, which is characterized by $\bar{E}_{\bar{\nu}_e} = (15.9 \pm 1.3) \text{ MeV}$ and $\bar{E}_{\nu_x}/\bar{E}_{\bar{\nu}_e} = 1.5 \pm 0.4$; although it well reproduces the LL model, the errors are still very large. Considering that many uncertainties concerning the SFR estimate possibly remain even in the future updated observations, the errors to these quantities would be much larger than the purely statistical ones given above.

5.3. Inverted Mass Hierarchy

Throughout the above discussions, we have assumed normal hierarchy of the neutrino masses ($m_1 \ll m_3$). However, the case of inverted mass hierarchy has not been experimentally excluded yet, and we explore such possibility in this subsection. In this case, flavor conversions inside the supernova envelope changes dramatically, compared with the normal mass hierarchy already discussed in §2.4. Since $\bar{\nu}_3$ is the lightest, $\bar{\nu}_e$ are created as $\bar{\nu}_3$, owing to large matter potential. In that case, it is well known that at a so-called resonance point, there occurs a level crossing between $\bar{\nu}_1$ and $\bar{\nu}_3$ (for more detailed discussions, see, e.g., Dighe & Smirnov 2000). At this resonance point, complete $\bar{\nu}_1 \leftrightarrow \bar{\nu}_3$ conversion occurs when the so-called adiabaticity parameter is sufficiently small compared to unity (it is said that resonance is nonadiabatic), while never occurs when it is large (adiabatic resonance). The adiabaticity parameter γ is quite sensitive to the value of θ_{13} , i.e., $\gamma \propto \sin^2 2\theta_{13}$; when $\sin^2 2\theta_{13} \gtrsim 10^{-3}$ ($\sin^2 2\theta_{13} \lesssim 10^{-5}$), the resonance is known to be completely adiabatic (nonadiabatic) (Dighe & Smirnov 2000). When the resonance is completely nonadiabatic (due to small θ_{13}), the situation is the same as in the case of normal mass hierarchy already discussed in §2.4 (because $\bar{\nu}_e$ at production become $\bar{\nu}_1$ at the stellar surface), and the $\bar{\nu}_e$ spectrum after oscillation is represented by equation (7). On the other hand, adiabatic resonance (due to large θ_{13}) forces $\bar{\nu}_e$ at production to become $\bar{\nu}_3$ when they escape from the stellar surface and therefore, the observed $\bar{\nu}_e$ spectrum is given by

$$\frac{dN_{\bar{\nu}_e}}{dE_{\bar{\nu}_e}} = |U_{e3}|^2 \frac{dN_{\bar{\nu}_e}^0}{dE_{\bar{\nu}_e}} + (1 - |U_{e3}|^2) \frac{dN_{\nu_x}^0}{dE_{\nu_x}} \simeq \frac{dN_{\nu_x}^0}{dE_{\nu_x}}. \quad (9)$$

The second equality follows from the fact that the value of $|U_{e3}|^2$ is constrained to be much smaller than unity from reactor experiment (Apollonio et al. 1999). Thus, equation (9) indicates that complete conversion takes place between $\bar{\nu}_e$ and ν_x . When the value of θ_{13} is large enough to induce adiabatic resonance ($\sin^2 2\theta_{13} \gtrsim 10^{-3}$), the obtained SRN flux and spectrum should be very different from ones obtained in §3.1 and §3.2. The SRN flux and event rate in this case were calculated with equations (3) and (9), and the results are summarized in the lower part of Table 2. The values (with the LL model) shown in this table is consistent with the previous calculation by Ando & Sato (2003a), in which a numerically calculated conversion probabilities were adopted with some specific oscillation parameter sets (that include a model with inverted

mass hierarchy and $\sin^2 2\theta_{13} = 0.04$) as well as realistic stellar density profiles.

The total flux becomes $9.4\text{--}14 \text{ cm}^{-2} \text{ s}^{-1}$, somewhat smaller than the values given in the upper part of the same table, because the total flux is dominated by low energy region. The flux at $E_\nu > 19.3 \text{ MeV}$ are enhanced to be $0.30\text{--}0.94 \text{ cm}^{-2} \text{ s}^{-1}$, but all of which is still below the current 90% C.L. upper limit $< 1.2 \text{ cm}^{-2} \text{ s}^{-1}$ obtained by the SK observation. The event rate at future detectable energy range, $E_\nu > 10 \text{ MeV}$, is expected to become $1.6\text{--}3.8 \text{ yr}^{-1}$, which is considerably larger than the values in the case of normal mass hierarchy, $0.97\text{--}2.3 \text{ yr}^{-1}$. The increase (decrease) of the flux and event rate integrated over high (total) energy region is due to the very high efficiency of the flavor conversion, $\nu_x \rightarrow \bar{\nu}_e$, inside the supernova envelope; because the original ν_x are expected to be produced with larger average energy as shown in Table 1, the efficient conversion makes the SRN spectrum harder, which enhances the flux and event rate at high energy region. Thus, if the inverted mass hierarchy as well as the large value for θ_{13} were realized in nature, the SRN detection would be rather easier compared with the other cases. Although we do not repeat such MC simulations that were introduced in §4, results can be easily inferred; the statistical errors in this case would be $\sim (3.8/2.3)^{1/2} = 1.3$ times smaller than the values given in Table 3, because they are inversely proportional to the square root of the event number.

6. CONCLUSIONS

In the present paper, we investigated the flux and event rate of SRN, and discussed their implications for the cosmic SFR. Since SRN is diffuse neutrino background emitted from past core-collapse supernova explosions, it contains fruitful information on not only the supernova neutrino spectrum itself, but also supernova rate in the past and present universe, which is quite difficult to estimate because, e.g., the problem of dust extinction is nontrivial. As reference models, we adopted the supernova rate model based on recent SFR observations (4), and supernova neutrino spectrum numerically calculated by three groups (LL; TBP; KRJ). As a result of our calculation, the flux integrated over the entire energy region was found $12\text{--}16 \text{ cm}^{-2} \text{ s}^{-1}$, depending on the adopted supernova neutrino spectrum (Table 2). Although there is no energy window for the SRN detection at present owing to various background events, in the near future, it is expected that the energy region of $10\text{--}30 \text{ MeV}$ is utilized for the SRN detection. This is due to the technique of neutron capture by dissolved Gd. In the detection energy range $E_e > 10 \text{ MeV}$, the SRN event rate was found to be $0.97\text{--}2.3 \text{ yr}^{-1}$ at the detector with fiducial volume of 22.5 kton (Table 2).

We also simulated the expected signal with one set of the reference models, by using the Monte Carlo method, and then analyzed these pseudo-data with several free parameters, obtaining one set of best fit values for them. Repeated 10^3 MC

simulations gave the independent 10^3 best fit parameter sets, and using their distribution we did statistical discussions. First of all, we used parametrization such that $R_{\text{SN}}(z) = R_{\text{SN}}^0(1+z)^\alpha$, where R_{SN}^0 and α are free parameters, assuming the supernova neutrino spectrum and luminosity are well understood by a future galactic supernova neutrino burst or future development of the numerical supernova simulations. The obtained distribution for these two parameters was found to be represented by $\alpha = 2.7 \pm 0.8$ (2.5 ± 0.2), $\delta\alpha/\langle\alpha\rangle = 30\%$ (7.8%) and $R_{\text{SN}}^0 = 1.2 \pm 0.4$ (1.0 ± 0.1) [$10^{-4} \text{ yr}^{-1} \text{ Mpc}^{-3}$], $\delta R_{\text{SN}}^0/\langle R_{\text{SN}}^0 \rangle = 28\%$ (7.7%) for the detector with effective volume of $22.5 \text{ kton} \cdot 5 \text{ yr}$ ($440 \text{ kton} \cdot 5 \text{ yr}$), in the case of the other parameter is fixed (Figs. 7 and 8; Table 3). The parametrized supernova rate model with the obtained parameter values are compared with the assumed reference model in Fig. 9, and we found that the fitting model well reproduced the reference model. On the other hand, if we fix neither values for these two parameters, the expected errors become rather large as $\delta\alpha/\langle\alpha\rangle = 37\%$ and $\delta R_{\text{SN}}^0/\langle R_{\text{SN}}^0 \rangle = 55\%$ even with effective volume of $440 \text{ kton} \cdot 5 \text{ yr}$.

In addition, we explored several other possibilities in §5. First, we discussed the dependence of the event number on the adopted lower cutoff energy. Although below 10 MeV there is a background of reactor neutrinos, their flux strongly depends on the detector sites, and the lower energy threshold E_{th} could possibly be reduced. We investigated the expected event number for $E_{\text{th}} < E_e < 30 \text{ MeV}$ as a function of E_{th} in Fig. 11 for various toy models of supernova rate, and found that the model that produces larger number of supernovae at $z > 1$ is satisfactorily distinguishable in the case of sufficiently small E_{th} . Secondly, the SRN spectrum as a potential probe of the supernova neutrino spectrum itself was investigated, because such an approach might be very important in the case of no galactic supernova explosions in the near future or no successful numerical supernova simulations. We discussed using the same MC procedure, but assuming the supernova rate is quite well understood. Although the obtained distribution reproduces properties of the LL spectrum, the errors were found to be still large, and considering the uncertainties concerning the SFR, these errors are only lower limit; the actual errors would be much larger. Finally, the case of the inverted mass hierarchy was investigated. We showed that only in the case that $\sin^2 2\theta_{13} \gtrsim 10^{-5}$, the values of SRN flux should be modified. Results with the case of completely adiabatic resonance, which realizes when $\sin^2 2\theta_{13} \gtrsim 10^{-3}$, are shown in the lower part of Table 2. In this case, it was found that the expected event rate would be enhanced to be $1.6\text{--}3.8 \text{ yr}^{-1}$, although these values are still below the current upper bound; the SRN detection could be more probable in this case.

This work was supported by Grant-in-Aid for JSPS Fellows.

REFERENCES

- Ando, S. 2003, Phys. Lett. B, 570, 11
 Ando, S. & Sato, K. 2003a, Phys. Lett. B, 559, 113
 —. 2003b, JCAP, 10, 001
 Ando, S., Sato, K., & Totani, T. 2003, Astropart. Phys., 18, 307
 Apollonio, M. et al. 1999, Phys. Lett. B, 466, 415
 Barr, G., Gaisser, T. K., & Stanev, T. 1989, Phys. Rev. D, 39, 3532
 Beacom, J. F. & Vagins, M. R. 2003, preprint (hep-ph/0309300)
 Bionta, R. M. et al. 1987, Phys. Rev. Lett., 58, 1494
 Connolly, A., Szalay, A., Dickinson, M., Rao, M. S., & Brunner, R. 1997, ApJ, 486, L11
 Cowie, L., Songaila, A., Hu, E., & Cohen, J. 1996, AJ, 112, 839
 Dighe, A. S. & Smirnov, A. Yu. 2000, Phys. Rev. D, 62, 033007
 Flores, H. et al. 1999, ApJ, 517, 148
 Fukugita, M. & Kawasaki, M. 2003, MNRAS, 340, L7
 Gaisser, T. K., Stanev, T., & Barr, G. 1988, Phys. Rev. D, 38, 85
 Gallego, J., Zamorano, J., Aragón-Salamanca, A., & Rego, M. 1995, ApJ, 455, L1
 Glazebrook, K., Blake, C., Economou, F., Lilly, S., & Colless, M. 1999, MNRAS, 306, 843

- Gronwall, C. 1998, in *Dwarf Galaxies and Cosmology*, ed. T. Thuan (Editions Frontières) astro-ph/9806240
- Hargrove, C. K., Blevins, I., Paterson, D., & Earle, E. D. 1995, *Nucl. Instrum. Methods A*, 357, 157
- Hartmann, D. H. & Woosley, S. E. 1997, *Astropart. Phys.*, 7, 137
- Hirata, K. et al. 1987, *Phys. Rev. Lett.*, 58, 1490
- Hughes, D. H. et al. 1998, *Nature*, 394, 241
- Kaplinghat, M., Steigman, G., & Walker, T. P. 2000, *Phys. Rev. D*, 62, 043001
- Keil, M. T., Raffelt, G. G., & Janka, H. T. 2003, *ApJ*, 590, 971
- Lilly, S., Fèvre, O. L., Hammer, F., & Crampton, D. 1996, *ApJ*, 460, L1
- Madau, P., della Valle, M., & Panagia, N. 1998a, *MNRAS*, 297, 17
- Madau, P., Ferguson, H. C., Dickinson, M. E., Giavalisco, M., Steidel, C. C., & Fruchter, A. 1996, *MNRAS*, 283, 1388
- Madau, P., Pozzetti, L., & Dickinson, M. 1998b, *ApJ*, 498, 106
- Malaney, R. A. 1997, *Astropart. Phys.*, 7, 125
- Malek, M. et al. 2003, *Phys. Rev. Lett.*, 90, 061101
- Pascalelle, S. M., Lanzetta, K. M., & Fernandez-Soto, A. 1998, *ApJ*, 508, L1
- Porciani, C. & Madau, P. 2001, *ApJ*, 548, 522
- Sawicki, M. J., Lin, H., & Yee, H. K. C. 1997, *AJ*, 113, 1
- Somerville, R. S., Primack, J. R., & Faber, S. M. 2001, *MNRAS*, 320, 504
- Steidel, C. C., Adelberger, K. L., Giavalisco, M., Dickinson, M., & Pettini, M. 1999, *ApJ*, 519, 1
- Strigari, L. E., Kaplinghat, M., Steigman, G., & Walker, T. P. 2003, preprint (astro-ph/0312346)
- Strumia, A. & Vissani, F. 2003, *Phys. Lett. B*, 564, 42
- Thompson, T. A., Burrows, A., & Pinto, P. 2003, *ApJ*, 592, 434
- Totani, T. & Sato, K. 1995, *Astropart. Phys.*, 3, 367
- Totani, T., Sato, K., Dalhed, H. E., & Wilson, J. R. 1998, *ApJ*, 496, 216
- Totani, T., Sato, K., & Yoshiii, Y. 1996, *ApJ*, 460, 303
- Tresse, L. & Maddox, S. 1998, *ApJ*, 495, 691
- Treyer, M., Ellis, R., Milliard, B., Donas, J., & Bridges, T. 1998, *MNRAS*, 300, 303
- Vogel, P. & Beacom, J. F. 1999, *Phys. Rev. D*, 60, 053003